FULL PAPER

Dalton
www.rsc.org/dalton

Peroxomolybdate(VI)–citrate and –malate complex interconversions by pH-dependence. Synthetic, structural and spectroscopic studies†‡

Zhao-Hui Zhou,* Shu-Ya Hou and Hui-Lin Wan*
Department of Chemistry and State Key Laboratory for Physical Chemistry of Solid Surface, Xiamen, China. E-mail: zhzhou@xmu.edu.cn; Fax: +86 592 2183047; Tel: +86 592 2184531

Received 25th November 2003, Accepted 10th March 2004
First published as an Advance Article on the web 29th March 2004

The reaction of potassium molybdate(VI) with biologically relevant ligands, citric and malic acids, in the presence of H_2O_2 was investigated for the effect of pH variations on the product pattern. That with citric acid led to the formation of the monomeric complex $K_4[MoO(O_2)_2(cit)]\cdot 4H_2O$ (**1**) in the pH range 7–9, and dimer $K_5[MoO(O_2)_2(Hcit)H(Hcit)(O_2)_2OMo]\cdot 6H_2O$ (**2**) (H_4cit = citric acid) at pH 3–6 through carboxylate–carboxylic acid hydrogen bonding. The relation with the previously identified $K_4[MoO_3(cit)]\cdot 2H_2O$ (**4**) and $K_4[Mo_2O_5(Hcit)_2]\cdot 4H_2O$ (**5**) were shown. These and other intermediates were shown to react in the pH range 3–6 to give a more stable species **2**; the reaction sequence was demonstrated either by the protonation from **1** or the deprotonation of $[MoO(O_2)_2(H_2cit)]^{2-}$ (**8**). Evidence that **2** exists as a dimer in solution is presented. The reaction with (*S*)-malic acid afforded Δ-$K_{2n}[MoO(O_2)_2((S)\text{-Hmal})]_n\cdot nH_2O$ (**3**) (H_3mal = malic acid) that was oxidized further to oxalato molybdate (**11**) by H_2O_2. The three complexes **1**–**3** were characterized by elemental analysis, UV, IR and NMR spectroscopies, in addition to the X-ray structural studies that show citrate and malate being coordinated as bidentate ligands *via* α-alkoxyl and α-carboxylate groups. The formation of these complexes is dictated by pH and their thermal stabilities varied with the coordinated hydroxycarboxylate ligands.

1 Introduction

The chemistry of transition metal peroxo complexes has received special attention due to their importance in a variety of industrial, pharmaceutical and biological processes.[1] They are widely used in stoichiometric as well as catalytic oxidation in organic and bio-chemistry,[2] for example in the oxidation of thioanisole,[3,4] methylbenzenes,[5] tertiary amines, alkenes, alcohols,[6,7] and bromide,[8] and also in olefin epoxidations.[9–17] They also act as isomerization catalysts for some allylic alcohols,[18] and have been applied in bleaching processes.[19,20] The reactivity of peroxo complexes depends on both the number and nature of auxiliary ligands.

A variety of peroxomolybdates coordinated with oxygen and nitrogen donors have been characterized structurally,[21–32] and studied in solution and the solid state.[33–39] For good reasons hydroxycarboxylic acids are frequently used as active coordinating agents; they exist widely in biological media, and have been known to influence strategic metabolic pathways governing the physiological activities of cells and multicellular organisms. Indeed, some peroxomolybdates(VI) carrying a hydroxycarboxylate ligand have been reported; they include monomeric citrate and glycolate complexes, $K_2[MoO(O_2)_2(H_2cit)]\cdot 3H_2O\cdot 0.5H_2O_2$,[40,41] $K_2[MoO(O_2)_2(glyc)]\cdot 2H_2O$, $(NH_4)_2[MoO(O_2)_2(glyc)]\cdot 0.5EtOH$ (H_2glyc = glycolic acid),[42] and dimeric tartrate complexes $K_4[Mo_2O_2(O_2)_4((R,R)\text{-tart})]\cdot 4H_2O$ and $(CN_3H_6)_4[Mo_2O_2(O_2)_4((R,R)\text{-tart})]\cdot 2H_2O$ (H_4tart = tartaric acid).[43]

Citrate ions are omnipresent small molecules in most plants and animal tissues where they regulate fundamental physiological processes, and are intermediates in carbohydrate metabolism, *e.g.* in the 'Krebs cycle'. Although a citrato peroxo molybdate(VI) has been reported,[40] our study in this field has been undertaken in order to answer one fundamental question; that is, can a pH variation act as the sole factor to induce structural changes in isolatable complexes in a hydrogen peroxide solution containing both molybdate(VI) and citrate ions? In essence, the question is whether the pH control of such a solution can dictate the fate of the reaction between the two reactants under oxidative conditions.[44]

Malate ions also play a significant role in metabolic pathways of plants and animals; for example they participate in the citric acid cycle, malate–aspartate shuttle, and others. A peroxo molybdenum malate has been studied by IR, Raman and nuclear magnetic resonance (NMR) spectroscopy,[38] and is reported to serve as an intermediate in the conversion of peroxo oxalato molybdate(VI).[45] Our work here, however, demonstrates that (*S*)-malate can remain unchanged, retaining its chirality, in an aqueous peroxo molybdenum(VI) solution at a specified pH range. Herein, two peroxo citrato complexes, $K_4[MoO(O_2)_2(cit)]\cdot 4H_2O$ (**1**) and $K_5[MoO(O_2)_2(Hcit)H(Hcit)(O_2)_2OMo]\cdot 6H_2O$ (**2**), and the malato complex Δ-$K_{2n}[MoO(O_2)_2((S)\text{-Hmal})]_n\cdot nH_2O$ (**3**) were synthesized and characterized. Their crystal structures and physical properties were reported.

2 Experimental

All experiments were carried out in the open air. All chemicals were analytical reagents and used without further purification. Nanopure-quality water was used throughout this work. Peroxide analyses were performed by permanganate titration.[46]

Preparation of $K_4[MoO(O_2)_2(cit)]\cdot 4H_2O$ (1)

Excess 30% hydrogen peroxide (1 ml) was added dropwise to a solution containing citric acid (0.84 g, 4 mmol) and one equivalent of potassium molybdate (1.31 g, 4 mmol). The resulting reaction mixture was adjusted to pH 8 with potassium hydroxide solution (1 M) until the color of the solution turned red. The aqueous solution, on standing in a refrigerator, turned yellow in one day, and gradually deposited light yellow crystals. After several days these crystals were collected and washed with ethanol to give **1** (1.28 g, 61%). CH elemental and peroxide analyses for $C_6H_{12}K_4MoO_{16}$: found (calc.): C 12.0 (12.2); H, 2.2 (2.0); O_2^{2-}, 11.2 (10.8%). UV-Vis spectrum: ε_{309} = 839 L mol^{-1} cm^{-1}. IR (KBr): ν_{as}(C=O) 1649s, 1576vs, ν_s(C=O) 1442m, 1425m, 1384s, ν(Mo=O) 946vs, ν(O–O) 853vs, ν_{asym}Mo(O–O)

† Electronic supplementary information (ESI) available: UV-Vis, IR spectra, TG and DSC analyses. See http://www.rsc.org/suppdata/dt/b3/b315280d/
‡ Dedicated to Prof. Khi-Rui Tsai on the occasion of his 90th birthday.

DOI: 10.1039/b315280d

650s, ν_sMo(O–O) 577s cm^{-1}. ^{1}H NMR (500 MHz): δ_H 2.845 (d, 2H, *J* 13 Hz, CH_2), 2.754 (d, 2H, *J* 13 Hz, CH_2). ^{13}C NMR: δ_C 188.5 $(CO_2)_\alpha$, 181.6 $(CO_2)_\beta$, 89.9 (≡CO), 51.0 (=CH_2).

Preparation of $K_5[MoO(O_2)_2(Hcit)H(Hcit)(O_2)_2OMo]\cdot 6H_2O$ (2)

Citric acid (0.84 g, 4 mmol) and an equal mole equivalent of potassium molybdate (1.31 g, 4 mmol) were dissolved in 5 ml water, to which excess 30% hydrogen peroxide (1 ml) was added dropwise. Potassium hydroxide (1 M) was added to give a yellow solution of pH 4. After being kept in a refrigerator for several days, light yellow crystals were obtained and were washed with ethanol to give **2** (1.34 g, 65%). CH elemental and peroxide analyses for $C_{12}H_{23}K_5Mo_2O_{30}$: found (calc.): C 13.9 (13.9); H, 2.3 (2.2); O_2^{2-}, 12.9 (12.4%). UV-Vis spectrum: ε_{307} = 776 L mol^{-1} cm^{-1}. IR (KBr): ν_{as}(C=O) 1722s, 1645vs, ν_s(C=O) 1438m, 1392s, 1342m, ν(Mo=O) 942s, ν(O–O) 857s, ν_{as}Mo(O–O) 647s, ν_sMo(O–O) 582m cm^{-1}. ^{1}H NMR (500 MHz): δ_H 2.780 (d, 2H, *J* 15 Hz, CH_2), 2.680 (d, 2H, *J* 15 Hz, CH_2). ^{13}C NMR: δ_C 186.0 $(CO_2)_\alpha$, 178.2 $(CO_2)_\beta$, 87.5 (≡CO), 47.8 (=CH_2).

Preparation of Δ-$K_{2n}[MoO(O_2)_2((S)\text{-Hmal})]_n\cdot nH_2O$ (3)

An aqueous solution of (*S*)-malic acid (0.54 g, 4 mmol) was slowly added to a stirred solution of potassium molybdate (1.31 g, 4 mmol), followed by excess 30% hydrogen peroxide (1 ml) added dropwise to afford a yellow solution of pH 4. To induce precipitation, ethanol (95%) was added dropwise until a permanent turbidity was obtained. The ethanol solution was kept in a refrigerator for two days to give light yellow crystals, which were filtered off and washed with ethanol to give **3** (0.77 g, 48%). CH elemental analysis and peroxide analyses for $C_4H_6K_2MoO_{11}$: found (calc.): C 11.9 (11.9); H, 1.7 (1.5); O_2^{2-}, 15.1 (15.8%). UV-Vis spectrum: ε_{306} = 700 L mol^{-1} cm^{-1}. CD: λ = 243 nm, $[\theta]_{221}$ = 3380. Optical rotation: $[\alpha]_D^{20}$ = −38°. IR (KBr): ν_{as}(C=O) 1701s, 1585vs, ν_s(C=O) 1417s, 1304s, ν(Mo=O) 947vs, ν(O–O) 859vs, ν_{as}Mo(O–O) 639s, ν_sMo(O–O) 576s cm^{-1}. ^{1}H NMR (500 MHz): δ_H 5.115 (dd, *J* 4, 1 Hz, HCO, 1H), 2.903 (dd, *J* 15.5, 1 Hz, CH_2), 2.798 (dd, *J* 15.5, 4 Hz, CH_2). ^{13}C NMR: δ_C 186.3 $(CO_2)_\alpha$, 178.2 $(CO_2)_\beta$, 81.6 (≡CO), 43.7 (CH_2).

Transformations of $K_4[MoO_3(cit)]\cdot 2H_2O$ (4) to 1 and 2

Excess 30% hydrogen peroxide (0.5 ml) was added to an aqueous solution of citrato molybdate(VI) **4** (1.05 g, 2 mmol), prepared as described previously.[44] Potassium hydroxide (1 M) was then added to bring the solution pH to 8. The solution was kept in a refrigerator for three days to deposit yellow crystals of **1** (0.74 g, 70%). The same procedure was followed except that the pH was adjusted to 4 to give **2** (0.84 g, 81%). The IR spectra were identical with the authentic samples **1** and **2**.

Transformation of $K_4[Mo_2O_5(Hcit)_2]\cdot 4H_2O$ (5) to 2

Excess 30% hydrogen peroxide (0.5 ml) was added to an aqueous solution of oxocitrato molybdate **5** (0.21 g, 0.23 mmol)[44] to give a solution of pH 3. The solution was kept in a refrigerator for two days to give yellow crystals of **2** (0.05 g, 20%).

Transformation of 1 to 2

Excess 30% hydrogen peroxide was added to an aqueous solution (5 ml) of peroxo citrato molybdate(VI) **1** (0.53 g, 1 mmol). Hydrochloric acid (1 M) was added dropwise to the solution to lower the pH to 4. The solution was kept in a refrigerator to afford yellow crystals of **2** (0.34 g, 67%).

Transformation of $K_2[Mo_2O_3(O_2)_4(H_2O)_2]\cdot 4H_2O$ (6) to 2

Dimeric peroxo molybdate(VI) **6** (0.53 g, 1 mmol), prepared by the published method,[22] was dissolved in 5 ml water. To this solution citric acid (0.42 g, 2 mmol) was added followed by a small amount of 30% H_2O_2. The resulting mixture was stirred and brought to pH 4 with potassium hydroxide (1 M). After keeping in a refrigerator for two days, yellow crystals **2** were obtained (1.03 g, 89%).

Transformation of $K_2[MoO(O_2)_2(H_2cit)]\cdot 0.5H_2O_2\cdot 3H_2O$ (8) to 2

Peroxo hydrogen citrato molybdate(VI) (**8**) (0.16 g, 0.2 mmol) prepared by potassium molybdate, citric acid and excess 30% hydrogen peroxide in an acid solution (pH = 1), was dissolved in 5 ml water. Potassium hydroxide (1 M) was added dropwise to the solution to pH 4. The solutions were kept in a refrigerator to afford yellow crystals of **2** (0.08 g, 61%). IR (KBr) for complex **8**: ν_{as}(C=O) 1705s, 1677vs, 1652vs, ν_s(C=O) 1426m, 1330s, 1251vs, ν_s(Mo=O) 966vs, ν(O–O) 849vs, ν_{as}Mo(O–O) 650s, ν_sMo(O–O) 574m cm^{-1}.

Physical measurements

Infrared spectra were recorded as Nujol mulls between KBr plates using a Nicolet 360 FT-IR spectrometer. Electronic spectra in water were recorded on a UV 2501 spectrophotometer. Elemental analyses were performed using an EA 1110 elemental analyzer. Optical rotations were measured with a Perkin-Elmer 341 automatic polarimeter. ^{1}H and ^{13}C NMR spectra were recorded in D_2O on a Varian UNITY 500 NMR spectrometer using DSS (sodium 2,2-dimethyl-2-silapentane-5-sulfonate) as the internal reference. Circular dichroism (CD) analyses were performed using a JASCO J-810 spectrometer. Thermogravimetric (TG) and differential thermal analysis (DTA) were carried out using a NETZSCH STA 449C thermal analyser.

X-Ray structure determination

Diffraction data were collected on a Bruker Smart Apex CCD diffractometer with graphite monochromated Mo-Kα radiation at 296 K. The structures were solved by SHELXS97 and refined by full-matrix least-squares procedures with anisotropic thermal parameters for all the non-hydrogen atoms; H atoms were located from difference Fourier maps. All calculations were performed on a microcomputer using SHELXL97 and SHELXS97 programs.[47,48]

CCDC reference numbers 225098–225100.

See http://www.rsc.org/suppdata/dt/b3/b315280d/ for crystallographic data in CIF or other electronic format.

3 Results and discussion

Various pathways leading to peroxo citrato molybdate(VI) $K_4[MoO(O_2)_2(cit)]\cdot 4H_2O$ (**1**) and $K_5[MoO(O_2)_2(Hcit)H(Hcit)(O_2)_2OMo]\cdot 6H_2O$ (**2**) are summarized in Scheme 1; the anions are shown corresponding to compound numbers, which represent both in this description. The scheme illustrates the sensitivity of the reaction toward pH in aqueous solutions containing potassium molybdate, potassium citrate and excess hydrogen peroxide. When pH 7–9 was maintained, such a solution showed an intermediary red color and slowly deposited **1** in 61% yield; the red intermediate was assumed to be the peroxo species $[Mo(O_2)_4]^{2-}$ **7**.[49] In contrast when the pH was adjusted to 2–6, such a solution yielded dimer **2** obviously through the intermediacy of diperoxo species **6**; this is supported by the ready conversion of **6** to **2** at pH 2–6 by citric acid under comparable conditions in a near quantitative yield.

Alternately, complexes **1** and **2** were prepared by the reaction of H_2O_2 with trioxocitrato molybdate $K_4[MoO_3(cit)]\cdot 2H_2O$ **4**, which was isolated from a solution of potassium molybdate and citric acid at pH 8.0–8.5. The reaction revealed its remarkable sensitivity to the pH control; **4** gave **1** at pH 8, but **2** at pH 4. Further, the dimeric citrato molybdate, $K_4[Mo_2O_5(Hcit)_2]\cdot 4H_2O$ (**5**), was converted by H_2O_2 to **2** at pH = 3. Both

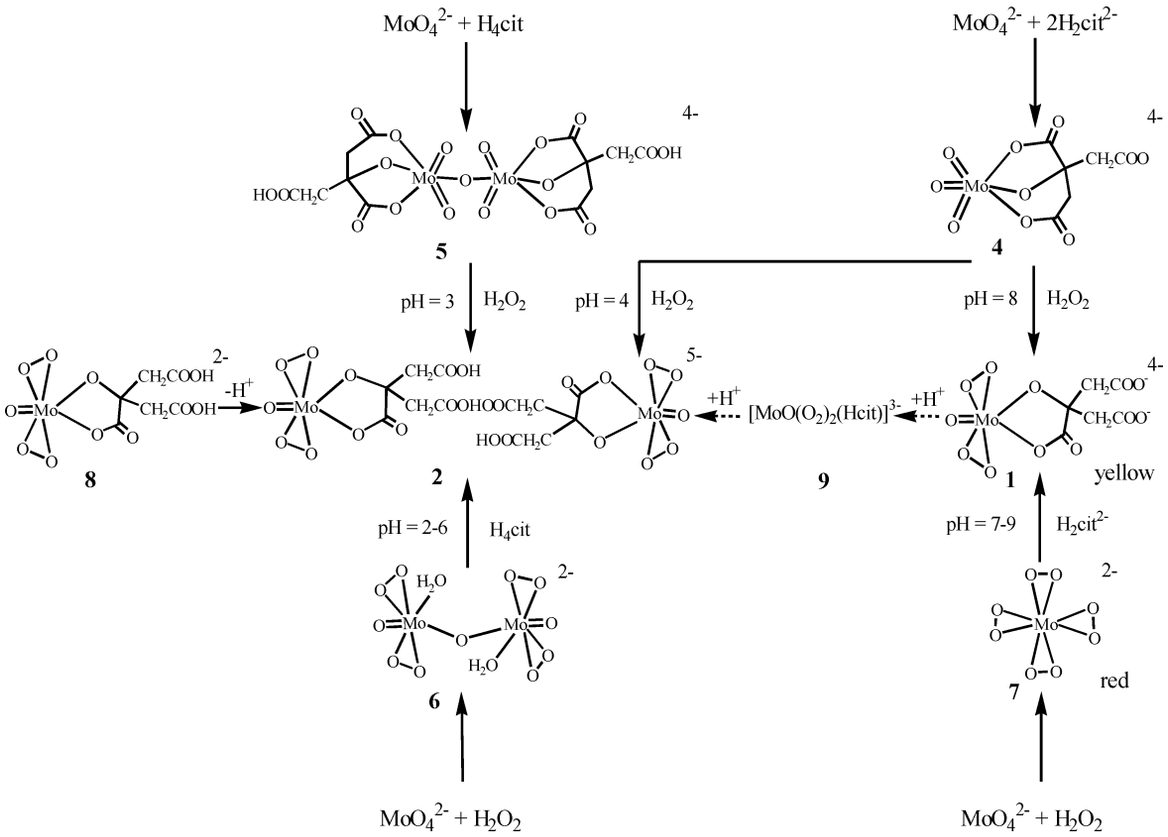

Scheme 1 Synthesis and transformation of peroxo citrato molybdates.[22,40,44]

oxo molybdates **4** and **5** were prepared and identified previously; these reactions show that their tridentate citrate ligand can be transformed to a more stable bidentate citrate ligand in peroxo molybdates **1** or **2**. This is a clear demonstration that the β-carboxylates in **4** and **5** are relatively weakly coordinated and detached by substitution of a peroxo group to give a more stable five-membered ring at pH 8 or 3–4 to afford **1** or **2**, respectively.

The structures of peroxo molybdates **1** and **2** were determined by single crystal X-ray crystallography and the ORTEP diagrams and pertinent crystal data are given in Figs. 1 and 2 and Tables 1 and 2, respectively. While the data will be discussed later, it is most significant that **2** is a centrosymmetric dimer formed through the linear hydrogen bonding of a β-carboxylate to a β-carboxylic acid group [O ··· O = 2.497(5) Å, O–H–O = 180.0°(3)]. The closest analogies are the crystal structures of potassium hydrogen bisphenylacetate and chloromaleate, both of which show intramolecular symmetrical and shortest col-

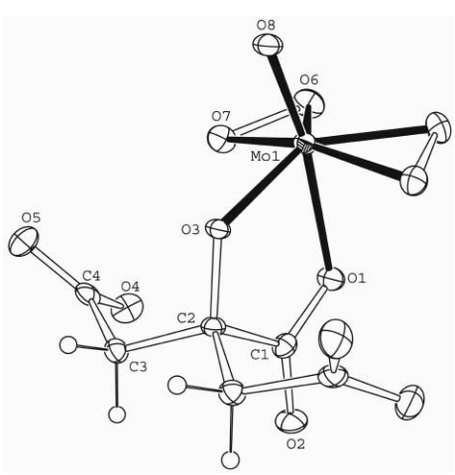

Fig. 1 Perspective view of the anion structure of $K_4[MoO(O_2)_2(cit)]\cdot 4H_2O$ (**1**).

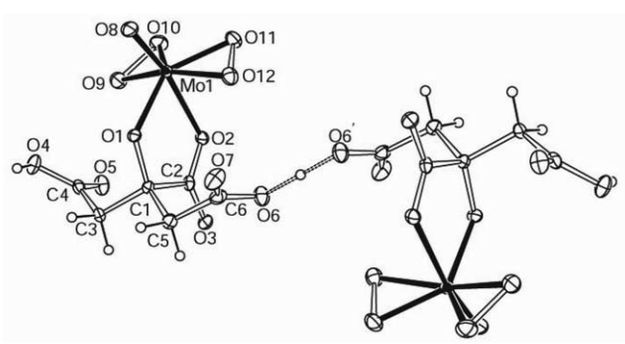

Fig. 2 Perspective view of the anion structure of $K_5[MoO(O_2)_2(Hcit)H(Hcit)(O_2)_2OMo]\cdot 6H_2O$ (**2**).

linear O–H–O linkages (2.437 and 2.445 Å).[50,51] The hydrogen bonding in **2** must be extraordinarily strong in view of its intermolecular mode, and in consideration of the intramolecular hydrogen bonding distance [O ··· O = 2.636(7) Å] in salicylic acid,[52] and the ordinary OH bond of 0.96 Å. This, in turn, reveals the extraordinary stability of dimer **2**, that is also experimentally demonstrated, firstly, by its formation and deposition, from **1**, in aqueous solution of pH 4, and secondly, by the inability of **2** to revert to **1** at pH 7–9. Under the forcing conditions at a higher pH, all the species decompose to potassium molybdate. These observations are a clear indication that **2** exists as a dimer not only in the crystalline state but also in solution through linear hydrogen-bonding.

It follows that there should exist, from **1**, a half protonated peroxo citrato molybdate species, $[MoO(O_2)_2(Hcit)]^{3-}$ (**9**), which was rapidly scavenged by **1** to form **2**, and could not be isolated. This mechanistic proposal was collaborated by the opposite approach to gain **2** starting from the anion of $K_2[MoO(O_2)_2(H_2cit)]\cdot 3H_2O\cdot 0.5H_2O_2$ (**8**), where both uncoordinated terminal carboxylates are protonated and the total charge of the anion is 2−. We prepared **8** *in situ* from peroxo molybdate **6** and citric acid in a pH 1 aqueous solution (*vide*

Table 1 Crystal data, intensity data collection and structure refinement for $K_4[MoO(O_2)_2(cit)]\cdot 4H_2O$ (**1**), $K_5[MoO(O_2)_2(Hcit)H(Hcit)(O_2)_2OMo]\cdot 6H_2O$ (**2**) and $K_{2n}[MoO(O_2)_2(S\text{-Hmal})]_n\cdot nH_2O$ (**3**)

Empirical formula	$C_6H_{12}K_4MoO_{16}$	$C_{12}H_{23}K_5Mo_2O_3$	$C_4H_6K_2MoO_{11}$
M_r	592.50	1034.68	404.23
Crystal color, habit	Light yellow, block	Light yellow, needle	Light yellow, needle
Crystal system, space group	Orthorhombic, *Pnma*	Triclinic, $P\bar{1}$	Monoclinic, $P2_1$
Unit cell dimensions:			
a/Å	22.361(2)	7.9131(5)	7.2393(6)
b/Å	10.3537(8)	9.4755(6)	10.7555(9)
c/Å	7.8268(6)	11.3561(7)	7.5130(6)
α/°		72.314(1)	
β/°		77.384(1)	94.408(2)
γ/°		72.276(1)	
V/Å^3	1812.1(2)	765.26(8)	583.1(1)
Z	4	1	2
D_c/g cm^{-3}	2.172	2.245	2.302
F(000)	1176	514	396
Diffractometer	Smart Apex CCD		
Radiation (*λ*/Å)	Mo-Kα (0.7107)		
T/°C	23		
Flack parameter[60]			−0.06(6)
GOF on F^2	1.01	1.04	1.031
R_1 ($I > 2\sigma(I)$)	0.031	0.035	0.035
wR_2 ($I > 2\sigma(I)$)	0.075	0.090	0.078
R_1 (all data)	0.042	0.037	0.036
wR_2 (all data)	0.079	0.091	0.079

Table 2 Selected bond distances (Å) and angles (°) for $K_4[MoO(O_2)_2(cit)]\cdot 4H_2O$ (**1**)

Mo(1)–O(1)	2.232(3)	Mo(1)–O(3)	1.971(2)	Mo(1)–O(6)	1.933(2)
Mo(1)–O(7)	1.985(2)	Mo(1)–O(8)	1.688(3)		
O(1)–Mo(1)–O(3)	75.0(1)	O(1)–Mo(1)–O(6)	86.0(1)	O(1)–Mo(1)–O(7)	81.8(1)
O(1)–Mo(1)–O(8)	168.2(1)	O(3)–Mo(1)–O(6)	133.3(1)	O(3)–Mo(1)–O(7)	90.4(1)
O(3)–Mo(1)–O(8)	93.3(1)	O(6)–Mo(1)–O(6^a)	85.8(1)	O(6)–Mo(1)–O(7)	44.3(1)
O(6)–Mo(1)–O(7^a)	129.0(1)	O(6)–Mo(1)–O(8)	102.6(1)	O(7)–Mo(1)–O(7^a)	162.7(1)
O(7)–Mo(1)–O(8)	98.6(1)				

Symmetry transformation: a x, $-y + 1/2$, z.

infra), wherein the solution pH was adjusted to 2–6 to afford **2** in good yields. The latter step obviously involved the formation of half de-protonated species **9**, and the rapid reaction of its β-carboxylate with a β-carboxylic acid group of **8**; **9** was not isolated in this attempt. Naturally at the higher pH, 7–9, **8** was directly de-protonated to **1**, without the intermediary of **2** through fast proton transfer.

The pH control was also critical in the formation and transformation of peroxo malato molybdate(VI) **3**. The reaction of potassium molybdate, (*S*)-malic acid and excess hydrogen peroxide in aqueous solution at pH 4–6 gave **3**. The corresponding deprotonated species $[MoO(O_2)(mal)]^{3-}$ might be formed in solution at higher pH, but decomposed to peroxo molybdates on attempted isolation. In the crystalline form, protonated species **3** has the high stability of a polymeric suprastructure, which is similar to the (*S*)-malato tungstate, (*S*)-malato molybdate and nitrilotriacetato tungstate[53–55] reported previously. At pH < 3, **3** was oxidatively cleaved to peroxo oxalato molybdate $K_2[MoO(O_2)_2(ox)]$ through a malate ⟶ oxalate catalytic reaction.[45]

Crystallographic data for the three compounds are summarized in Table 1. The structure of the anion of complex **1** is shown in Fig. 1. The molybdenum is coordinated by a terminal oxo group, two bidentate peroxo groups and a bidentate citrate ligand binding through its α-alkoxyl atom and α-carboxylate group. The coordination about the molybdenum is essentially pentagonal bipyramidal, similar to that found in the peroxo carboxylate ligand molybdate(VI).[40,42,43] The axial positions are taken up by the oxo ligand [Mo–O 1.688(3) Å] and the oxygen atom from the α-carboxylate group. The equatorial positions are occupied by the two bonded peroxo groups and deprotonated α-alkoxyl group [Mo–O 1.971(2) Å]. The strong *trans*-influence of the terminal oxo group results in the long distance of Mo–O of the α-carboxylate group [Mo–O 2.232(3) Å] at the opposing axial positions. It is recognized that the η^2-O_2^{2-} ligand is a π-donor like the oxoligand,[25] thus each peroxo and oxo ligand in this case are in *cis* configuration to interact with different metal orbitals.

An ORTEP diagram of the anion of **2** is shown in Fig. 2. Each molybdenum atom is also seven-coordinate with pentagonal bipyramidal geometry as for complex **1**. The citrate ion acts as a bidentate ligand with the α-alkoxyl and α-carboxylate oxygen coordinated to the molybdenum atom, while one of the β-carboxylate groups is free to bind as a centrosymmetric dimer through a linear $[CO_2^- \cdots HO_2C]$ hydrogen bonding. That is, one of the β-carboxylates of a citrate unit is bonded to a β-carboxylic acid group of another unit.

As shown in Table 3, the Mo–O distances in complex **2** vary systematically. The distance of the double bond Mo=O is 1.684(2) Å. The Mo–O(peroxo) bond distances are in the range 1.926(3)–1.980(2) Å, suggesting that they are asymmetrically bonded. The Mo–O(alkoxyl) bonds are slightly longer [2.034(2) Å], indicating the deprotonation of the hydroxyl group. The Mo–O(carboxylate) bonds are the longest [2.196(2) Å], and comparable with the length of Mo–O(alkoxyl) [2.185 and 2.251 Å] and Mo–O(carboxylate) [2.180 and 2.312 Å] of a coordinated homocitrate and citrate ligand in MoFe protein and their *nifV* multant complexes in *Klebsiella pneumoniae*.[56,57]

The X-ray structure of peroxo malato molybdate(VI) **3** consists of discrete anions, potassium cations, and water molecules. As shown in Fig. 3, the coordination mode about each molybdenum atom is the same as that in peroxo citrato molybdate(VI). The α-alkoxyl ligand oxygen is coplanar with the four peroxo oxygens. The molybdenum is displaced by about 0.28 Å out of the plane, toward the "oxo' oxygen. The bipyramid has the oxo oxygen and the α-carboxylate oxygen atom at the axial positions.

Table 3 Selected bond distances (Å) and angles (°) for $K_5[MoO(O_2)_2(Hcit)H(Hcit)(O_2)_2OMo]\cdot 6H_2O$ (**2**)

Mo(1)–O(1)	2.034(2)	Mo(1)–O(2)	2.197(2)	Mo(1)–O(8)	1.684(2)
Mo(1)–O(9)	1.975(3)	Mo(1)–O(10)	1.926(3)	Mo(1)–O(11)	1.930(2)
Mo(1)–O(12)	1.980(2)				
O(1)–Mo(1)–O(2)	74.18(8)	O(1)–Mo(1)–O(8)	91.7(1)	O(1)–Mo(1)–O(9)	90.1(1)
O(1)–Mo(1)–O(10)	133.7(1)	O(1)–Mo(1)–O(11)	133.6(1)	O(1)–Mo(1)–O(12)	90.3(1)
O(2)–Mo(1)–O(8)	165.9(1)	O(2)–Mo(1)–O(9)	81.6(1)	O(2)–Mo(1)–O(10)	87.7(1)
O(2)–Mo(1)–O(11)	87.0(1)	O(2)–Mo(1)–O(12)	80.81(9)	O(8)–Mo(1)–O(9)	99.8(1)
O(8)–Mo(1)–O(10)	103.2(1)	O(8)–Mo(1)–O(11)	102.6(1)	O(8)–Mo(1)–O(12)	98.6(1)
O(9)–Mo(1)–O(10)	44.6(1)	O(9)–Mo(1)–O(11)	129.1(1)	O(9)–Mo(1)–O(12)	161.6(1)
O(10)–Mo(1)–O(11)	85.8(1)	O(10)–Mo(1)–O(12)	129.1(1)	O(11)–Mo(1)–O(12)	44.4(1)
O(6)–H ··· O(6)[a]	2.497(5)	O(6)–H ··· O(6)[a]	180.0(3)		

Symmetry transformation: a $1-x, 1-y, -z$.

Table 4 Selected bond distances (Å) and angles (°) for $K_{2n}[MoO(O_2)_2(S\text{-Hmal})]_n\cdot nH_2O$ (**3**)

Mo(1)–O(1)	2.011(4)	Mo(1)–O(2)	2.277(4)	Mo(1)–O(6)	1.972(4)
Mo(1)–O(7)	1.942(4)	Mo(1)–O(8)	1.942(3)	Mo(1)–O(9)	1.967(4)
Mo(1)–O(10)	1.693(4)				
O(1)–Mo(1)–O(2)	74.5(1)	O(1)–Mo(1)–O(6)	87.5(2)	O(1)–Mo(1)–O(7)	130.9(2)
O(1)–Mo(1)–O(8)	133.1(2)	O(1)–Mo(1)–O(9)	88.9(2)	O(1)–Mo(1)–O(10)	93.4(2)
O(2)–Mo(1)–O(6)	78.0(2)	O(2)–Mo(1)–O(7)	84.1(2)	O(2)–Mo(1)–O(8)	86.0(2)
O(2)–Mo(1)–O(9)	79.5(2)	O(2)–Mo(1)–O(10)	167.8(2)	O(6)–Mo(1)–O(7)	44.5(2)
O(6)–Mo(1)–O(8)	130.1(2)	O(6)–Mo(1)–O(9)	157.3(2)	O(6)–Mo(1)–O(10)	101.2(2)
O(7)–Mo(1)–O(8)	87.4(2)	O(7)–Mo(1)–O(9)	130.3(2)	O(7)–Mo(1)–O(10)	103.9(2)
O(8)–Mo(1)–O(9)	45.1(2)	O(8)–Mo(1)–O(10)	103.3(2)	O(9)–Mo(1)–O(10)	101.4(2)
O(4)–H ··· O(3)[a]	2.597(6)	O(4)–H ··· O(3)[a]	177(8)		

Symmetry transformation: a $x, y, 1+z$.

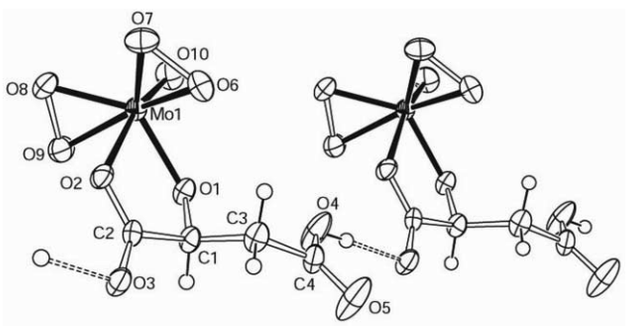

Fig. 3 Perspective view of the anion structure of $K_{2n}[MoO(O_2)_2((S)\text{-Hmal})]_n\cdot nH_2O$ (**3**).

While a malate ion serves as a tridentate ligand in many peroxo malato vanadate(v) complexes,[58,59] in this complex it employs the α-alkoxyl and α-carboxylate groups to coordinate in bidentate mode so as to form a five-membered ring with the molybdenum, the other uncoordinated β-carboxylate group remaining protonated. In the solid state, the chirality of the whole complex is induced by the chiral ligand. An enantioselective aggregation with homochirality ··· ΔΔΔ ··· for **3** is obtained within a one dimensional catenarian chain through strong hydrogen bonding [O ··· O = 2.597(6) Å] (Table 4), which results in the formation of a homochiral supramolecular framework. This strong hydrogen bonding of the type O–H ··· O involves the oxygen O4 of the uncoordinated carboxylate OH group and O3 of the carbonyl entity; the pattern is different from that of $\Lambda\text{-}Na_{3n}[MoO_2H((S)\text{-mal})_2]_n$.[50] It should be added that the driving force for such strong hydrogen bonding in **3** as well as in **2** is not clear at this stage.

Table 5 shows comparisons of Mo–O distances. When compared with other mononuclear oxomalate molybdate compounds, the Mo–O distances of α-alkoxyl and α-carboxylate of the malate in complex **3** is the longest. The oxoperoxo malato and oxoperoxo citrato complexes show longer Mo–O(alkoxyl) and Mo–O(carboxylate) than the corresponding bidentate oxocitrate molybdate. Complexes **3** and **2** possess the longest Mo–O of carboxylate and alkoxyl bonds among the peroxo complexes due to their special polymer or dimer configuration.

In the crystalline form, complex **3** is less stable than complexes **1** and **2**. While peroxo citrato complexes **1** and **2** remain unchanged for months if they are pure and are kept under dry atmosphere, peroxo malato complex **3** changes in two days under comparable conditions. Crystals of these peroxo complexes are soluble in water and show a broad peroxo → molybdenum charge transfer band at about 310 nm in their UV spectra. Complex **3** shows an enhanced rotation power of ($[\alpha]_D^{20} = -38°$) in comparison to (*S*)-malic acid ($[\alpha]_D^{20} = -27°$), and in circular dichroism (CD) spectra in water a band at 221 nm is observed with molecular ellipticity $[\theta]_{221} = 3380$, the latter originating from the chiral malate ligand bonded to the metal. These results lead us to conclude that complex **3** has a chiral metal center.

IR spectra of the complexes display characteristic features of the coordinated citrato or malato ligand and of the oxo and peroxo groups. Specifically, absorptions for antisymmetric stretching carboxylate vibrations ν_{as}(COOH) and ν_{as}(COO) appear at 1649 and 1575 for **1**, 1722 and 1645 for **2**, and 1701 and 1585 for **3**, and of symmetric stretching vibrations ν_s(COO) at 1440–1300 cm^{-1} for all compounds. The frequencies of the coordinated carboxylate are shifted to lower values compared to those of the free ligands. The Mo=O vibration occurs as sharp bands at 946, 942 and 947 cm^{-1} for complexes **1**, **2** and **3**, respectively. The ν(O–O) vibration occurs as a clearly defined strong bond around 860 cm^{-1}, occurring at a higher frequency compared to that around 800 cm^{-1} in the spectra of simple peroxide salts. Additional bands in the 650–570 cm^{-1} range belong to ν_{as}Mo(O–O) and ν_sMo(O–O). In an allied study, the isolated complex[41] was alleged to have the structure $K_2[MoO(O_2)_2(H_2cit)_2]\cdot 0.5H_2O\cdot 3H_2O$ (**8**). On the basis of their IR spectrum being identical with complex **2** in the present study, the previous complex[41] must be revised to complex **2** rather than **8**. We have prepared **8** and its IR spectrum has been recorded (*vide supra*).

Table 5 Comparisons of Mo–O distances (Å) in citrato or malato complexes

Complex	Mo–O(α-alkoxyl)	Mo–O(α-carboxylate)	Ref.
$K_2[MoO(O_2)_2(glyc)]\cdot 2H_2O$	1.991(5)	2.239(6)	42*a*
$(NH_4)_2[MoO(O_2)_2(glyc)]\cdot 0.5EtOH$	1.974(2), 2.011(2)	2.310(2), 2.211(2)	42*b*
$K_4[Mo_2O_2(O_2)_4(tart)]\cdot 4H_2O$	1.962(7)	2.248(7)	43*a*
$(CN_3H_6)_4[Mo_2O_2(O_2)_4((R,R)\text{-tart})]\cdot 2H_2O$	1.98(2)	2.26(2)	43*b*
$Cs_2[MoO_2(Hmal)_2]\cdot H_2O$	1.939(8)	2.243(9)	61
$Na_{3n}[MoO_2H((S)\text{-mal})_2]_n$	1.935(2)	2.182(3)	54
$K_2[MoO(O_2)_2((S)\text{-Hmal})]\cdot H_2O$ (**3**)	2.011(4)	2.277(4)	This work
$Na_2[MoO_2(H_2cit)]\cdot H_2O$	1.960(7), 1.953(6)	2.190(7), 2.247(6)	62
$K_2[MoO(O_2)_2(H_2cit)]\cdot 3H_2O\cdot 0.5H_2O_2$ (**8**)	2.011(7)	2.220(8)	40
$K_5[MoO(O_2)_2(Hcit)H(Hcit)(O_2)_2OMo]\cdot 6H_2O$ (**2**)	2.034(2)	2.197(2)	This work
$K_4[MoO(O_2)_2(cit)]\cdot 4H_2O$ (**1**)	1.971(2)	2.232(3)	This work
$[MoFe_7S_9N((R)\text{-homocit})(N\text{-his})]$	2.185	2.180	56
$[MoFe_7S_9(cit)(N\text{-his})]$	2.251	2.312	57

Owing to some dissociation on dissolving in H_2O (D_2O), the ^{13}C NMR spectra of **1**–**3** showed additional small peaks in Fig. 4, but the major peaks can be interpreted. Complexes **1** and **2** show a sharp AB quartet for the methylene protons of the coordinated citrate ligand in their ^1H NMR spectra. Complex **1** shows large lower field shifts of some ^{13}C resonances through coordination in comparison with the corresponding carbons in K_3Hcit ion at a similar pH (7.5), *e.g.* the shift of the α-alkoxyl carbon ($\Delta\delta$ ~14.3 ppm) at 89.9 ppm and α-carboxylate groups ($\Delta\delta$ ~ 6.3 ppm) at 188.5 ppm. The differences of ^{13}C signals of **2** in comparison with KH_3cit ion at a similar pH (3.4) clearly show that both α-alkoxyl ($\Delta\delta$ ~ 12.1 ppm) and α-carboxylate ($\Delta\delta$ ~ 8.4 ppm) groups are coordinated.

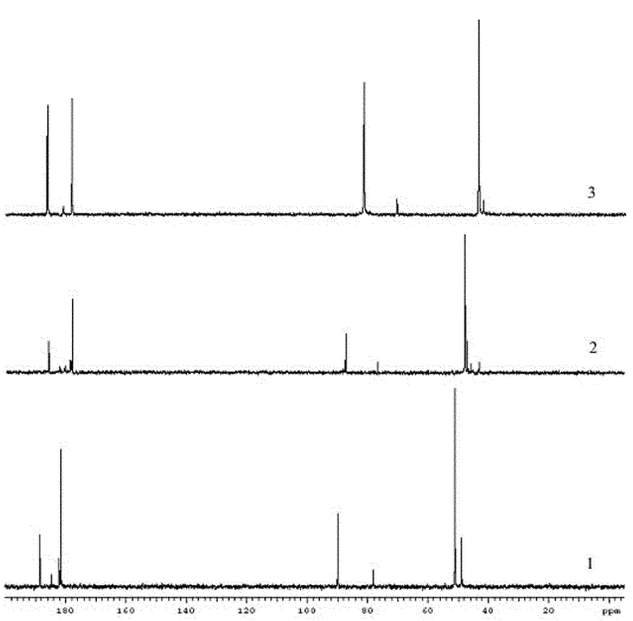

Fig. 4 ^{13}C NMR spectra of the peroxo citrato and malato complexes: bottom, $K_4[MoO(O_2)_2(cit)]\cdot 4H_2O$ (**1**); middle, $K_5[MoO(O_2)_2(Hcit)H(Hcit)(O_2)_2OMo]\cdot 6H_2O$ (**2**); top, $K_{2n}[MoO(O_2)_2((S)\text{-Hmal})]_n\cdot nH_2O$ (**3**).

In the malato complex **3**, the ^{13}C signal of α-carboxylate and α-alkoxyl shifted greatly to a lower field ($\Delta\delta = 9.3$ and 14.4 ppm) compared to that of (*S*)-malic acid, implying the involvement of coordination. The ^1H NMR spectrum of **3** shows two quartets around 2.9 ppm and a quartet at δ 5.115 ppm. These shifts occur at lower fields when compared to those of the free ligand.

Complexes **1**, **2** and **3** dissolve in D_2O emitting bubbles and thus ^1H and ^{13}C spectra display several additional peaks derived from the liberated ligand in addition to the signals of the complexes themselves.

Thermogravimetric (TG) and differential scanning calorimetric analyses (DSC) carried out for these compounds under N_2 atmosphere indicate that different ligands in the peroxo complexes lead to different thermal stabilities. The first decomposition in complex **1** occurring at 120 °C is associated with the loss of the four H_2O molecules, followed by the loss of the peroxo groups at 191 °C. Complex **2** also undergoes several decomposition steps. The loss of four H_2O occurs at 98.7 °C followed by the next two decomposition stages at 173 and 192 °C. The separation of these latter stages was too close to allow the weight loss to be determined exactly at each step. However, the total weight loss could be attributed to the loss of another two H_2O molecules and the peroxo groups. The situation of complex **3** is different from the above two complexes, which decomposed explosively at 140 °C. The decomposition results in a sharp loss of mass and absence of peroxide as confirmed by the TG curves.

Acknowledgements

We thank the Ministry of Science & Technology (G1999022408, 001CB108906) and the National Science Foundation of China (20021002, 29933040) for the generous support of this research, and Professor Yuan L. Chow for stimulating discussions and many suggestions.

References

1 K. Sato, M. Aoki and R. Noyori, *Science*, 1998, **281**, 1646–1647.
2 B. Tamami and H. Yeganeh, *Eur. Polym. J.*, 1999, **35**, 1445–1550.
3 M. Chiarini, N. D. Gillitt and C. A. Bunton, *Langmuir*, 2002, **18**, 3836–3842.
4 C. A. Bunton and N. D. Gillitt, *J. Phys. Org. Chem.*, 2002, **15**, 29–35.
5 R. Bandyopadhyay, S. Biswas, S. Guha, A. K. Mukherjee and R. Bhattacharyya, *Chem. Commun.*, 1999, 1627–1628.
6 O. Bortolini, S. Campestrini, F. D. Furia and G. Modena, *J. Org. Chem.*, 1987, **52**, 5467–5469.
7 A. J. Bailey, W. P. Griffith and B. C. Parkin, *J. Chem. Soc., Dalton Trans.*, 1995, 1833–1837.
8 M. S. Reynolds, S. J. Morandi, J. W. Raebiger, S. P. Melican and S. P. E. Smith, *Inorg. Chem.*, 1994, **33**, 4977–4984.
9 K. A. Jøgensen, *Chem. Rev.*, 1989, **89**, 431–458.
10 M. J. Morris, *Coord. Chem. Rev.*, 1996, **152**, 309–358.
11 G. Wahl, D. Kleinhenz, A. Schorm, J. Sundermeyer, R. Stowasser, C. Rummey, G. Bringmann, C. Fichert and W. Kifer, *Chem. Eur. J.*, 1999, **5**, 3237–3251.
12 R. J. Cross, P. D. Newman, R. D. Peacock and D. Stirling, *J. Mol. Catal. A: Chem.*, 1999, **144**, 273–284.
13 L. J. Csányi and K. Jáky, *J. Catal.*, 1999, **127**, 42–50.
14 D. V. Deubel, J. Sundermeyer and G. Frenking, *Inorg. Chem.*, 2000, **39**, 2314–2320.
15 C. D. Valentin, P. Gisdakis, I. V. Yudanov and N. Rösch, *J. Org. Chem.*, 2000, **65**, 2996–3004.
16 D. V. Deubel, J. Sundermeyer and G. Frenking, *J. Am. Chem. Soc.*, 2000, **122**, 10101–10108.
17 X. Y. Wang, H. C. Shi and S. Y. Xu, *J. Mol. Catal. A: Chem.*, 2003, **206**, 213–223.
18 F. R. Fronczek, R. L. Luck and G. Wang, *Inorg. Chem. Commun.*, 2002, **5**, 384–387.

19 K. M. Thompson, M. Spiro and W. P. Griffith, *J. Chem. Soc., Faraday Trans.*, 1996, **92**, 5235–5240.
20 F. Taube, M. Hashimoto, I. Andersson and L. Pattersson, *J. Chem. Soc., Dalton Trans.*, 2002, 1002–1008.
21 M. H. Dichman and M. T. Pope, *Chem. Rev.*, 1994, **94**, 569–584.
22 R. Stomberg, *Acta Chem. Scand.*, 1968, **24**, 1072–1090.
23 W. Shum, *Inorg. Chem.*, 1986, **25**, 4329–4330.
24 C. Djordjevic, J. L. Gundersen and B. A. Jacobs, *Polyhedron*, 1989, **8**, 541–543.
25 G. Ramakrishnan, P. S. Rao and S. Subramanian, *J. Chem. Soc., Dalton Trans.*, 1991, 185–3191.
26 W. P. Griffithm, A. M. Z. Slawin, K. M. Thompson and D. J. Williams, *J. Chem. Soc., Chem. Commun.*, 1994, 569–570.
27 P. Martín-Zarza, P. Gili, F. V. Rodríguez-Romero, C. Ruiz-Pérez and X. Solans, *Inorg. Chim. Acta*, 1994, **233**, 173–175.
28 R. J. Cross, L. J. Farrugia, P. D. Newman, R. D. Peacock and D. Stirling, *J. Chem. Soc., Dalton Trans.*, 1996, 4149–4150.
29 C. Djordjevic, N. Vuletic, B. A. Jacobs, M. Lee-Renslo and E. Sinn, *Inorg. Chem.*, 1997, **36**, 1798–1805.
30 F. R. Sensato, Q. B. Cass, E. Longo, J. Zukerman-Schpector, R. Custodio, J. Andrés, M. Z. Hernandes and R. L. Longo, *Inorg. Chem.*, 2001, **40**, 6022–6025.
31 M. J. Hinner, M. Grosche, E. Herdtweck and W. R. Thiel, *Z. Anorg. Allg. Chem.*, 2003, **629**, 2251–2257.
32 S. Y. Hou, Z. H. Zhou, H. L. Wan and S. W. Ng, *Inorg. Chem. Commun.*, 2003, **6**, 1246–1248.
33 M. C. Chakraborti, S. Ganguly and M. Bhattacharjee, *Polyhedron*, 1993, **12**, 55–58.
34 V. Nardello, J. Marko, G. Vermeersch and J. M. Aubry, *Inorg. Chem.*, 1995, **34**, 4950–4957.
35 M. L. Ramos, M. M. Calderia and V. M. S. Gil, *J. Chem. Soc., Dalton Trans.*, 2000, 2099–2103.
36 M. L. Ramos, M. M. Pereira, A. M. Beja, M. R. Silva, J. A. Paixão and V. M. S. Gil, *J. Chem. Soc., Dalton Trans.*, 2002, 2126–2231.
37 F. Taube, I. Andersson, I. Toth, A. Bodor, O. Howarth and L. Pettersson, *J. Chem. Soc., Dalton Trans.*, 2002, 4451–4456.
38 T. T. Bhengu and D. K. Sanyal, *Thermochim. Acta*, 2003, **397**, 181–197.
39 L. Pettersson, I. Andersson, F. Taube, I. Toth, M. Hashimoto and O. W. Howarth, *J. Chem. Soc., Dalton Trans.*, 2003, 146–152.
40 J. Flanagan, W. P. Griffith, A. C. Skapski and R. W. Wiggins, *Inorg. Chim. Acta.*, 1985, **96**, L23–L24.
41 A. A. Said, A. M. Al-Kority and E. M. Nour, *J. Phys. Chem. Solids*, 1992, **53**, 1245–1249.
42 (*a*) A. C. Dengel, W. P. Griffith, R. D. Powell and A. C. Skapski, *J. Chem. Soc., Dalton Trans.*, 1987, 991–995; (*b*) D. Bayot, B. Tinant and M. Devillers, *Inorg. Chim. Acta*, 2004, **357**, 809–816.
43 (*a*) A. C. Dengel, W. P. Griffith, R. D. Powell and A. C. Skapski, *J. Chem. Soc., Chem. Commun.*, 1986, 555–556; (*b*) B. Tinant, D. Bayot and M. Devillers, *Z. Kristallogr.*, 2003, **218**, 572–574.
44 Z. H. Zhou, H. L. Wan and K. R. Tsai, *Inorg. Chem.*, 2000, **39**, 59–64.
45 C. Djordjevic and K. J. Covert, *Inorg. Chim. Acta*, 1985, **101**, L37–L39.
46 J. S. Fritz and G. H. Schenk, *Quantitative Analytical Chemistry*, Allyn and Bacon, Boston, MA, 4th edn., 1987.
47 L. J. Farrugia, *J. Appl. Crystallogr.*, 1999, **32**, 837–838.
48 G. M. Sheldrick, SHELXL97 and SHELXS97, University of Göttingen, Germany, 1997.
49 S. E. Cremer and A. V. Subbaratnam, *Chem. Commun.*, 1967, 32–33.
50 A. D. Ellison and H. A. Levy, *Acta Crystallogr.*, 1965, **19**, 260–268.
51 G. Stomberg, *Acta Chem. Scand.*, 1969, **23**, 2755–2763.
52 G. E. Bacon and R. J. Jude, *Z. Kristallogr., Kristallgeom. Kristallphys. Kristallchem.*, 1973, **19**, 19–40.
53 Z. H. Zhou, G. F. Wang, S. Y. Hou, H. L. Wan and K. R. Tsai, *Inorg. Chim. Acta*, 2001, **314**, 184–188.
54 Z. H. Zhou, W. B. Yan, H. L. Wan and K. R. Tsai, *J. Inorg. Biochem.*, 2002, **90**, 137–143.
55 Z. H. Zhou, S. Y. Hou, Z. J. Ma, H. L. Wan and K. R. Tsai, *Inorg. Chem. Commun.*, 2002, **5**, 388–390.
56 O. Einsle, F. A. Tezcan, S. L. A. Andrade, B. Schmid, M. Yoshida, J. B. Howard and D. C. Rees, *Science*, 2002, **297**, 1696–1970.
57 S. M. Mayer, C. A. Gormal, B. E. Smith and D. M. Lawson, *J. Biol. Chem.*, 2002, **277**, 35263–35266.
58 C. Djordjevic, M. Lee-Renslo and E. Sinn, *Inorg. Chim. Acta.*, 1995, **233**, 97–102.
59 M. Kaliva, T. Giannadaki and A. Salifoglou, *Inorg. Chem.*, 2001, **40**, 3711–3718.
60 H. D. Flack, *Acta Crystallogr., Sect. A*, 1983, **39**, 876–881.
61 C. B. Knobler, A. J. Wilson, R. N. Hider, I. W. Jensen, B. R. Penfold, W. T. Robinson and C. J. Wilkins, *J. Chem. Soc., Dalton Trans.*, 1983, 1299–1303.
62 Z. H. Zhou, H. L. Wan and K. R. Tsai, *J. Chem. Soc., Dalton Trans.*, 1999, 4289–4290.